

Stable isotopes track the ecological and biogeochemical legacy of mass mangrove forest dieback in the Gulf of Carpentaria, Australia

Yota Harada¹, Rod M. Connolly¹, Brian Fry², Damien T. Maher^{3,4}, James Z. Sippo³, Luke C. Jeffrey³, Adam J. Bourke⁵, Shing Yip Lee⁶

5 ¹Australian Rivers Institute – Coast and Estuaries, and School of Environment and Science, Griffith University, Gold Coast, Queensland, Australia

²Australian Rivers Institute, Griffith University, Nathan, Queensland, Australia

³Southern Cross Geoscience, Southern Cross University, Lismore, New South Wales, Australia

⁴School of Environment, Science and Engineering, Southern Cross University, Lismore, NSW, Australia

10 ⁵College of Engineering, Information Technology and the Environment, Charles Darwin University, Northern Territory, Australia

⁶Simon F.S. Li Marine Science Laboratory, School of Life Sciences, and Earth System Science Programme, The Chinese University of Hong Kong, Shatin, Hong Kong SAR, China

Correspondence to: Yota Harada (yota.harada@griffithuni.edu.au)

15 **Abstract.** A combination of elemental analysis, bulk stable isotope analysis (bulk SIA) and compound-specific stable isotope analysis of amino acids (CSIA-AA) was used to assess and monitor carbon (C), nitrogen (N) and sulfur (S) cycling of a mangrove ecosystem that suffered mass dieback of trees in the Gulf of Carpentaria, Australia in 2015-16, attributed to an extreme drought event. Three field campaigns were conducted over a period from 2016 to 2018, at 8, 20 and 32 months after the event to obtain biological time-series data. Invertebrates and associated organic matter including mangroves, and sediments
20 from the impacted ecosystem showed enrichment in ¹³C, ¹⁵N and ³⁴S relative to those from an adjacent unimpacted reference ecosystem, likely indicating lower mangrove carbon fixation, lower nitrogen fixation and lower sulfate reduction in the impacted ecosystem. For example, invertebrates representing the feeding types of grazing, leaf feeding, and algae feeding were more ¹³C enriched at the impacted site, by 1.7 – 4.1‰ and these differences did not change over the period from 2016 to 2018. The CSIA-AA data indicated widespread ¹³C enrichment across five essential amino acids and all groups sampled (except
25 filter feeders) within the impacted site. The seedling density increased from 0.2 per m² in 2016 to 7.1 per m² in 2018 in the impacted forest, suggesting recovery of the vegetation. Recovery of CNS cycling, however, was not evident even after 32 months, suggesting a biogeochemical legacy of the mortality event. Continued monitoring of the post-dieback forest is required to predict the long-term trajectory of ecosystem recovery. This study shows that time-series SIA can track biogeochemical changes over time and evaluate recovery of an impacted ecosystem from an extreme event.

30

1 Introduction

Low frequency, high intensity weather events, such as droughts, tropical cyclones, heatwaves and climatic extremes can cause mass mortality of foundation species such as mangroves (Sippo et al., 2018), saltmarshes (Silliman et al., 2005), seagrasses (Thomson et al., 2015), kelps (Wernberg et al., 2016) and corals (Hughes et al., 2017). The frequency and intensity of extreme

35 climatic events are expected to increase due to climate change (Coumou and Rahmstorf, 2012; Stott, 2016). In 2015-16, an extensive area (>7000 ha) of mangrove forest along ~1,000 km of coastline in the Gulf of Carpentaria, Australia, experienced severe dieback, an event associated with the climatic extreme of drought (Duke et al., 2017; Sippo et al., 2020a). As mangroves show characteristics of pioneer species (Tomlinson, 2016), large-scale disturbances have likely played an important role in their evolution. However, the processes, rates and patterns of recovery from disturbances are still largely unknown. In most
40 cases, recovery of mangroves primarily relies on the recruitment of seedlings (Smith et al., 1994; Krauss and Osland, 2019). Disturbances in mangrove forests not only affect recruitment, but can also change the cycling of C, N and S. Loss of mangrove trees and root structures can change organic matter inputs, sediment oxygenation and degradation of sediment organic matter with consequences for benthic assemblages (Sweetman et al., 2010; Bernardino et al., 2018; Harada et al., 2019), coastal
45 carbon cycle (Jeffrey et al., 2019; Sippo et al., 2020b), sediment C and N stocks (Adame et al., 2018), microbial assemblages, and associated nutrient processes e.g. nitrogen fixation and sulfate reduction (Sjöling et al., 2005). Although mangroves can recover from mortality events, the rate of recovery can be slow. For example, a study of mangrove mortality attributed to an oil spill incident shows that full canopy recovery may take over 50 years (Connolly et al. 2020). Full recovery of belowground C and N stocks may take over 40 years after mangrove replantation (Adame et al., 2018).

50 Stable isotope analysis (SIA) provides biogeochemical process information integrated over time and is useful for environmental assessment and monitoring. As elements such as carbon (C), nitrogen (N) and sulfur (S) circulate in the biosphere, stable isotopic compositions of $^{13}\text{C}/^{12}\text{C}$, $^{15}\text{N}/^{14}\text{N}$ and $^{34}\text{S}/^{32}\text{S}$ can change in predictable ways due to mixing and fractionation, giving insights into sources and cycling of these elements (Fry 2006). SIA has been widely used in mangrove ecosystem studies to better understand food web interactions (Bouillon et al., 2008; Larsen et al., 2012; Bui and Lee, 2014;
55 Abrantes et al., 2015), nutrient uptake (McKee et al., 2002), water use (Santini et al., 2015; Hayes et al., 2019), cycling of C (Maher et al., 2013a; Maher et al., 2017; Sasmito et al., 2020), N (Fry and Cormier, 2011), S (Raven et al. 2019), and greenhouse gas emissions (Maher et al., 2013b). While traditional field methods such as measuring species composition to evaluate structure and functioning of ecosystems can be time-consuming and expensive, SIA of ecosystem components can evaluate functional aspects of element cycling and food webs in a cost-effective way (Fry, 2006). To quantify food web
60 dynamics, SIA of total organic matter (“bulk”) requires determination of the baseline isotope values of the food web, but this is difficult to achieve, particularly for complex detrital food webs. Some of the uncertainties associated with bulk SIA have been clarified by compound-specific isotope analysis of amino acids (CSIA-AA). This technique has been increasingly used to assess pathways of energy transfer throughout food webs by distinguishing the effects of baseline isotope values and trophic

transfer. Distinct isotopic fractionation between two groups of amino acids occurs with each trophic transfer. In general, non-
65 essential and/or trophic AAs show large isotopic fractionation per trophic step, while essential and/or source AAs show little fractionation, reflecting the baseline isotope values of the food web (Ishikawa et al., 2018; Larsen et al., 2013; Ohkouchi et al., 2017).

We investigated changes in C, N and S cycling associated with the Gulf of Carpentaria mangrove forest dieback (Duke et al.,
70 2017), using a combination of traditional ecological survey techniques, bulk SIA, and CSIA-AA of carbon. We hypothesised that the mortality of mangrove foundation species has changed the overall circulation of C, N and S elements and these biogeochemical changes would most likely be reflected in $\delta^{13}\text{C}$, $\delta^{15}\text{N}$ and $\delta^{34}\text{S}$ values of mangrove ecosystem components such as mangrove plants, sediment and associated animals. We also tested the hypothesis that these isotopic compositions changed over time with the recovery of mangrove vegetation. $\delta^{13}\text{C}$, $\delta^{15}\text{N}$ and $\delta^{34}\text{S}$ values were measured for samples including
75 mangroves, sediment and invertebrates collected in a comparative setting of impacted mangrove forest site and an adjoining unaffected reference forest site in the Gulf of Carpentaria, Australia.

2 Material and Methods

2.1 Study site

The Gulf of Carpentaria in tropical Northern Australia is an extensive, shallow coastal gulf. The area mainly consists of low-
80 lying wetlands and is largely inaccessible with little direct human activity. Mangroves are abundant in the area, but the dry climate limits the extent, diversity, and height of mangroves in the region (Asbridge et al., 2016). The wide tidal wetlands spread along the shoreline with high intertidal saltfans and saltmarsh covering more area than mangroves. Mangroves are often distributed in the seaward margin, typically as a narrow strip and fronted by extensive, shallow mudflats. The distribution of mangroves in this region is associated with tidal and freshwater inundation, river discharge and regular sediment supply
85 through freshwater input. Increased amounts of rainfall and associated flooding and sea level rise were responsible for recent mangrove extension in this region between 1987 and 2014 (Asbridge et al., 2016). *Avicennia marina* was the dominant mangrove species at the study site in Karumba, Gulf of Carpentaria (Fig 1A).

Over 7,000 ha of mangroves along ~ 1,000 km of the Gulf of Carpentaria coastline in Australia experienced mass mortality
90 during the summer in 2015-16, (Duke et al., 2017), the most extensive mangrove forest dieback ever recorded due to natural causes (Sippo et al., 2018). At the same time, there were coinciding mangrove mass mortality events in Exmouth, Western Australia (Lovelock et al., 2017) and Kakadu National Park, Northern territory (Asbridge et al., 2019). The climate in the Gulf region is wet-dry tropical with mean annual precipitation ranging from approximately 600 to 900 mm. Dry conditions prevail for six to eight months and most rainfall occurs between December and March (Bureau of Meteorology, see www.bom.gov.au).
95 The dieback coincided with a weak monsoon (low rainfall), combined with high vapor pressure deficit, and El Niño–Southern

Oscillation-induced low sea-levels (Duke et al., 2017; Lovelock et al., 2017; Harris et al., 2017). The drought conditions most likely caused accumulative hydric, thermal and radiant stresses (Duke et al., 2017). In addition to low water availability, iron (Fe) toxicity due to a rapid mobilisation of sedimentary Fe and regional variability in groundwater flows may have also played a role in the dieback (Sippo et al., 2020a). The event led to the widespread death of mangrove trees in the region providing an
100 unfortunate yet unique opportunity to test tree mortality effects on biogeochemical and ecological functioning of mangroves and capture recovery patterns.

Three field campaigns were conducted in August 2016 (8 months after the event), August 2017 (20 months after the event) and August 2018 (32 months after the event) in the winter dry-seasons in Karumba. Some local factors (e.g. river influence
105 and localised groundwater flow paths) may have kept some mangroves from dying back in the region. A forest that had suffered dieback (impacted) on the east of Norman River outlet and an adjoining unaffected forest (unimpacted) on the west, provided the setting for comparisons. In order to assess differences between the two forests (impacted vs. unimpacted), as well as to capture trends from across the intertidal zone and to ensure that the physical-oceanographic conditions between the two forests were as similar as possible, three sampling transects (2 to 2.5 km apart) were set for each forest with the length of each transect
110 being approximately 200 m (Fig. 1B, C). Each transect consists of six sampling plots (approx. 40m apart), namely forest edge (landward), high, mid, low, forest edge (seaward) and mudflat (Table 1). Samples from each plot were pooled for analysis. Due to logistical constraints and the presence of saltwater crocodiles, fieldwork was restricted to daytime, low tide and dry seasons.

2.2 Samples

115 Since our focus was to measure recovery of mangrove vegetation and food-web, we monitored mangrove sapling/seedlings and stable isotopes of invertebrates during the period from 2016 to 2018. Mangrove and sediment samples were also collected but they are limited to 2018 (Table 1). Some of the SIA samples including invertebrates, mangrove and sediment collected in 2017 were used to measure the initial dieback reported in Harada et al. (2019). During each field campaign, four common mangrove macroinvertebrate groups with different feeding modes were collected from each forest including a leaf-eating crab
120 (*Parasesarma molluccensis* and/or *Episesarma* sp.), an algae-eating (deposit-feeding) crab (*Tubuca signata*), a grazer gastropod (*Telescopium telescopium*) and a filter-feeding bivalve (*Saccostrea* sp, an oyster). For each feeding group, 3 to 5 individuals at each of the sampling transects (n=3) within the forest were collected and muscle tissues were pooled for SIA. In 2018, fully developed green leaves of *A. marina* were collected from at about 1 to 1.5 m height, from 3 to 5 individual trees (1 to 3 leaves per tree) at each sampling plot, stored in plastic containers, then composited. In the impacted site, leaves were
125 collected from regrowth of trees that had survived. Leaf samples were washed thoroughly, rinsed with distilled water and the main vein was removed. Additionally, wood samples (n=2, 5 to 25cm diameter) were collected using a hand saw from stems at chest height from the mid intertidal zone of each forest. Dead trees were sampled at the impacted site. Two to three bulk

SIA measurements were made from sapwood (2 to 3cm deep) of each sample and measurements were averaged. Wood samples were generally very low in S and not sufficient for $\delta^{34}\text{S}$ analysis.

130

In 2018, surface (<0.5 cm) sediments that represent the recent deposition and microphytobenthos (MPB) were collected along each transect. Additionally, subsurface (0.5 to 20 cm) sediment samples (n=6) that represent long-term averages were collected at the mid intertidal zone of each forest using a core sampler (5 cm in diameter and 20 cm deep). For $\delta^{13}\text{C}$ measurements, the sediment samples were acidified with 1M HCl to remove the inorganic fraction. Microphytobenthos (MPB) samples (n=6) 135 were separated from surface sediment collected at each forest. The separation was achieved through density gradient centrifugation in Ludox colloidal silica (Sigma) as described in Bui and Lee (2014). The MPB extraction was followed by microscopic examination to confirm that samples mostly contained green cells (i.e. diatoms and filamentous cyanobacteria). Additionally, surface sediment samples were collected from offshore (approx. 1km) using a grab sampler and from the adjacent saltpan (approx. 200m inland from the forest). Offshore water samples (n=3) were also collected and then filtered through 140 glass fiber filters (diameter 44mm, pore size 0.7 μm , Whatman GFF) to obtain particulate organic matter (POM), material such as phytoplankton that is transported to the mangrove.

To estimate mangrove seedling/sapling densities (ind. m^{-2}) from each forest and their changes over time, seedling/saplings were counted with a 50 x 50 cm quadrat at the mid intertidal zone. A photo was taken of each quadrat (for 2016, n=124 for the 145 unimpacted forest and n=143 for the impacted forest, for 2017, n=161 and n=175, and for 2018, n=80 and n=117, respectively) and then counts of seedlings and samplings were made in the laboratory. The seedlings/samplings were mostly *A. marina* but also include some *Aegiceras corniculatum*.

2.3 Stable isotope analysis

All invertebrate, leaf, sediment and filter samples were stored separately in sealed plastic containers at -20°C until analysis, 150 then dried at 60°C, powdered, homogenized and put in tin capsules for SIA. $\delta^{13}\text{C}$, $\delta^{15}\text{N}$ and $\delta^{34}\text{S}$ measurements were carried out on an elemental analyzer (Europa EA-GSL, Sercon) coupled to an isotope ratio mass spectrometer (Hydra 20-22, Sercon) at Griffith University, Brisbane, Australia. Isotope values are reported relative to Vienna Pee Dee Belemnite (PDB), atmospheric N₂(AIR), and Vienna Canyon Diablo Troilite (VCDT) for C, N and S, respectively. Harada et al. (2019), reported $\delta^{13}\text{C}$ and $\delta^{15}\text{N}$ values for some of the samples collected in 2017 from the same study location.

155

The samples collected in 2017 showed substantial differences in $\delta^{13}\text{C}$ values between the two forests (Harada et al., 2019) suggesting that they are representative of the dieback impact. The 2017 samples from each forest including the mangrove leaf (n=2), MPB (n=1), algae feeder (n=3), leaf feeder (n=2 to 3), grazer (n=3), filter feeder (n=2) were further measured for carbon isotopic composition of individual amino acids ($\delta^{13}\text{C}_{\text{AA}}$). 8 mg (for animal tissues) or 30 mg (for plant tissues) of sample 160 materials were transferred to borosilicate vials with heat and acid-resistant caps. They were then flushed with N₂ gas, sealed

and hydrolysed in 0.5mL (animal tissues) or 2mL (plant tissues) of 6M HCl at 150°C for 70 minutes, then dried in a heating block at 60°C under a stream of N₂ gas. The dried samples were derivatised by methoxycarbonylation as described by Walsh et al. (2014). Amino acid derivatives were separated by a Trace GC Ultra gas chromatograph (Thermo Scientific) using a DB-23 column, Agilent, 30m x 0.25mm, 0.25μm film at the stable isotope facility at the University of California (Davis, CA, USA). The GC was interfaced with a Delta V Plus isotope ratio mass spectrometer via a GC IsoLink (Thermo Scientific). L-Norleucine was used as an internal standard and to calculate provisional values. Pure AAs mixtures with calibrated δ¹³C were co-measured. One mixture was used for final calibration and others were for the scale normalisation standard and the primary quality assurance standard (unused in corrections). Two working standards were co-measured as secondary quality assurance materials. Exogenous carbon was accounted by the method detailed by Docherty et al. (2001). Following these processes, δ¹³C values were determined for 10 AAs (Gly, glycine; Asx, aspartic acid/asparagine; Pro, proline; Glx, glutamic acid/glutamine; Ala, alanine; Lys, lysine; Ile, isoleucine; Leu, leucine; Phe, phenylalanine; and Val, valine). Met, methionine; His, histidine; and Hyp, hydroxyproline were at or below the limit of quantitation (LOQ) for some samples. Since we were interested in δ¹³C values of essential amino acids (δ¹³C_{EAA}), δ¹³C values of Lys, Ile, Leu, Phe and Val were reported in the study.

2.4 Data analysis

All statistical analyses were undertaken in R version 3.4.3 with RStudio interface version 1.1.414. Differences among group means were explored with ANOVA, but for the count data i.e. seedling/ sampling populations, generalized linear model (GLM) with Poisson distribution was used. Before performing ANOVA, the assumptions of homogeneity of variance and normality were tested using Levene's and Shapiro-Wilk's tests, respectively. Two way ANOVA was used to test the effects of time (year) and forest type (unimpacted and impacted) on stable isotope values of invertebrates. To explore δ¹³C patterns among five EAAs, δ¹³C_{EAA} values were normalised to the respective sample means following the procedure of Larsen et al. (2009) as follows:

$$Norm(\delta_{EAA}) = \delta_{EAA} - \mu \quad (1)$$

where μ represents the mean value of all five EAAs (Ile, Leu, Lys, Phe and Val) in the sample. PERMANOVA was performed to test if the pattern of δ¹³C among five EAAs of samples differ between the forests. In this analysis, the normalized δ¹³C_{EAA} dataset was used and the Euclidean distance was used as distance metric. Permutation test of multivariate homogeneity of dispersions was performed to check whether dispersions around the centroids are similar between the two forests. All statistical tests used a significance criterion of α=0.05.

3 Results

3.1 Mangroves

In 2016, at the impacted site, mangrove seedling and sapling populations were lower than at the unimpacted site (GLM df = 1, estimate 3.75, p < 0.001) but significantly increased throughout the period from 2016 to 2018 (GLM df = 2, estimate 0.01,

p < 0.001; Fig. 2). C, N and S elemental compositions (%) of *A. marina*, did not differ significantly between the two sites, but the isotopic compositions varied significantly (Table 2). The $\delta^{13}\text{C}$ values (mean \pm SD) of green leaves harvested from *A. marina* trees, were significantly higher (i.e. more ^{13}C -enriched) in the impacted site ($-25.8 \pm 1.0\text{\textperthousand}$) than the unimpacted site ($-28.4 \pm 1.5\text{\textperthousand}$; ANOVA $F_{1,28} = 32.9$, p < 0.001; Fig. 3A, Table 2). The $\delta^{15}\text{N}$ values varied more in the impacted site (ranged from -0.9 to 6.7‰) than in the unimpacted site (ranged from 2.9 to 6.2‰; Fig. 3A). The $\delta^{34}\text{S}$ values were generally higher in the impacted site ($13.5 \pm 5.4\text{\textperthousand}$, range 7.7 to 23.3‰) than the unimpacted site ($12.6 \pm 5.6\text{\textperthousand}$, range 5.0 to 21.9‰). Leaf $\delta^{34}\text{S}$ values became more ^{34}S depleted from higher to lower intertidal zones in the impacted site (ANOVA $F_{4,10} = 5.56$, p = 0.013; Fig. 3B). This pattern was weaker in the unimpacted site, but leaf $\delta^{34}\text{S}$ values significantly varied across intertidal zones (ANOVA $F_{4,10} = 6.48$, p = 0.007; Fig. 3B). Leaf $\delta^{13}\text{C}$ and $\delta^{15}\text{N}$ values did not display such patterns along the intertidal zones (Table S2). Leaf C, N and S (%) did not show any clear trends among two forests and along transects. Yellow leaves generally had a higher S content (~1.2%) than green leaves (0.5 to 0.7%) (Table 2). Wood samples generally had very low N and S contents, significantly lower than the leaves.

3.2 Sediment

For the surface (<0.5 cm) sediment collected in 2018, TOC (%) differed significantly between the two forests with the values (mean \pm SD) of $2.02 \pm 1.16\%$ for the unimpacted site and $1.06 \pm 0.37\%$ for the impacted site (ANOVA $F_{1,28} = 12.75$, P = 0.001), suggesting that the surface sediment from the impacted site contains ~48% lower TOC relative to those of the unimpacted site (Table 3). The surface sediment TN (%) was also significantly lower for the impacted site (0.09 ± 0.03) than the unimpacted site ($0.15 \pm 0.06\%$; ANOVA $F_{1,28} = 9.32$, P = 0.005). TOC of mudflat (<0.5 cm) sediment collected adjacent to the two forests also differed significantly with those of impacted site being lower ($0.58 \pm 0.18\%$) than the unimpacted site ($1.02 \pm 0.08\%$; ANOVA $F_{1,4} = 14.54$, P = 0.019). TN (%) of mudflat (<0.5 cm) sediment was also significantly lower for the impacted site (ANOVA $F_{1,4} = 9.81$, P = 0.035). TOC (%) of 0.5 – 20 cm sediment did not differ significantly between the two sites with the values of $1.83 \pm 0.73\%$ for the unimpacted and $1.29 \pm 0.55\%$ for the impacted site (ANOVA $F_{1,10} = 2.07$, P = 0.181). TN (%) of 0.5 – 20 cm sediment also did not differ significantly between the two sites with the values of $0.09 \pm 0.03\%$ for the unimpacted and $0.12 \pm 0.04\%$ for the impacted site (ANOVA $F_{1,10} = 3.02$, P = 0.113). Despite the substantial variation in TOC and TN, the C/N ratio did not differ significantly between the two sites (ANOVA P > 0.05).

The $\delta^{13}\text{C}$ values of surface sediment differed significantly between the two sites with those from the impacted site showing higher values ($-21.8 \pm 1.0\text{\textperthousand}$) than those from the unimpacted site ($-24.3 \pm 1.2\text{\textperthousand}$; ANOVA $F_{1,28} = 22.48$, P < 0.001). This pattern was consistent across the intertidal zones with $\delta^{13}\text{C}$ values from the impacted site becoming similar to those from the adjacent mudflat (Fig. 4; Table S3). However, those of 0.5 to 20 cm sediment did not differ significantly with the values of $-24.4 \pm 0.5\text{\textperthousand}$ for the impacted site and $-25.2 \pm 0.9\text{\textperthousand}$ for the unimpacted site (ANOVA $F_{1,10} = 3.92$, P = 0.076). Surface sediment collected in the adjacent mudflat did not display a significant difference in $\delta^{13}\text{C}$ values between the two sites with the values

of $-21.2 \pm 0.9\text{\textperthousand}$ for those collected adjacent to the unimpacted forest and $-21.8 \pm 0.8\text{\textperthousand}$ for those collected adjacent to the impacted site (ANOVA $F_{1,4} = 0.64$, $P = 0.47$). The $\delta^{13}\text{C}$ value of the surface sediment ($-21.8 \pm 1.0\text{\textperthousand}$) in the impacted forest was similar to the value of those collected in the mudflat ($-21.2 \pm 0.9\text{\textperthousand}$) which were also similar to those collected from offshore ($-21.5 \pm 1.1\text{\textperthousand}$). Those $\delta^{13}\text{C}$ values also matched with the $\delta^{13}\text{C}$ value of POM collected offshore ($-21.5 \pm 1.5\text{\textperthousand}$). Surface sediment collected from adjacent unvegetated saltpan areas also showed similar values (Table 3). MPB extracted from the surface sediment showed significantly different $\delta^{13}\text{C}$ values between the impacted site ($-21.5 \pm 1.3\text{\textperthousand}$) and unimpacted site (- $25.2 \pm 1.0\text{\textperthousand}$; ANOVA $F_{1,10} = 28.53$, $P < 0.001$).

3.3 Fauna

CNS isotopic compositions of mangrove macroinvertebrates representing algae feeder, grazers and leaf feeders from the impacted site were more enriched in ^{13}C , ^{15}N and ^{34}S than their counterparts from the unimpacted forest throughout the period between 2016 and 2018 (Fig. 5). However, the filter feeding oyster that relies on water column organic matter showed relatively less difference between the two forests (Fig. 5). Overall, $\delta^{13}\text{C}$ values of the four feeding groups range from -23 to -15 \textperthousand for the unimpacted site and -20 to -14 \textperthousand for the impacted site. The $\delta^{15}\text{N}$ values ranged from 5.5 to 9.1 \textperthousand for the unimpacted site with the fauna in the impacted site having a slightly higher range of 5.6 to 9.5 \textperthousand . The $\delta^{34}\text{S}$ values ranged from 8.2 to 16 \textperthousand for the unimpacted site and 13.4 to 21.7 \textperthousand for the impacted site. The $\delta^{13}\text{C}$, $\delta^{15}\text{N}$ and $\delta^{34}\text{S}$ values of the algae feeder and the grazer significantly differed between the two forests (ANOVA $p < 0.05$). The $\delta^{13}\text{C}$ and $\delta^{34}\text{S}$ values of the leaf feeder significantly differed between the two forests (ANOVA $p < 0.05$), but the $\delta^{15}\text{N}$ values were not significantly different (ANOVA $F_{1,13} = 1.72$, $p = 0.212$). The filter feeder $\delta^{13}\text{C}$ values did not differ between the two forests (ANOVA $F_{1,8} = 1.719$, $p = 0.212$), but the $\delta^{15}\text{N}$ and $\delta^{34}\text{S}$ values differed significantly between the two forests (ANOVA $p < 0.05$). The effect of time was significant for the leaf feeder $\delta^{34}\text{S}$ values, the grazer $\delta^{15}\text{N}$ values, the filter feeder $\delta^{15}\text{N}$ and $\delta^{13}\text{C}$ values (ANOVA $p < 0.05$). In 2018, leaf feeder $\delta^{13}\text{C}$ values, grazer $\delta^{34}\text{S}$ values and algae feeder $\delta^{34}\text{S}$ values significantly differed between the impacted and unimpacted sites (Turkey post hoc test, $P < 0.05$), showing no recovery of the invertebrate fauna $\delta^{13}\text{C}$ and $\delta^{34}\text{S}$ status 32 months after the dieback event. However, $\delta^{15}\text{N}$ values became similar between the two forests in 2018 (Fig. 5).

3.4 Compound-specific isotope analysis of amino acid carbon

The samples collected in 2017 were further measured for carbon isotopic compositions in individual essential amino acids. $\delta^{13}\text{C}_{\text{EAA}}$ values corresponded to the bulk $\delta^{13}\text{C}$ values with the samples from the impacted site consistently showing higher values than those from the unimpacted forest (Table 4 and Fig 6). The pattern of normalized $\delta^{13}\text{C}$ among five EAAs (Lys, Ile, Val, Leu and Phe) for all the consumers did not differ between the two forests ($p > 0.05$; Table 4 and Fig S1). The $\delta^{13}\text{C}_{\text{EAA}}$ pattern of mangrove leaves did not differ between the forests, regardless of the substantial bulk isotope difference between the unimpacted ($-26.7 \pm 2.2\text{\textperthousand}$) and impacted ($-25.4 \pm 0.1\text{\textperthousand}$) (Table 4). This isotope pattern was similar for all four feeding groups as well as for the MPB samples (Fig. 6 and Fig S1).

4.1 Mangroves

The recovery of mangrove forests from tree mortality events caused by disturbances such as cyclones, generally relies upon the recruitment of seedlings (Smith et al., 1994; Krauss and Osland, 2019). Subsequently, degraded habitats with a reduced seed pool, production and delivery, e.g. by habitat fragmentation, may show slower forest recovery (Milbrandt et al., 2006).

260 The establishment of seedlings may also be inhibited by persistent inundation due to a decreased sediment elevation (Cahoon et al., 2003; Asbridge et al., 2018). Mangroves are resilient ecosystems and may recover quickly from natural disturbances (Sherman et al., 2001), but in some cases, full recovery may take decades (Imbert et al., 2000; Connolly et al., 2020). Further, mangrove degradation may be followed by fast colonisation of non-mangrove herbaceous species, e.g. succulent saltmarsh (Mbense et al., 2016; McKee et al., 2007; Rashid et al., 2009). However, this was not largely evident from our study site. In
265 both mangrove forests at the Gulf of Carpentaria site, the density of mangrove seedling/samplings significantly increased throughout the period from 2016 to 2018, suggesting that recovery was starting to occur in some areas within 32 months after the dieback and propagule pool was available in the vicinity. The increase in seedling/sampling density at the unimpacted site was unexpected, but this indicates that there was some stress at the unimpacted site during the dieback period and/or the temporal variability of seedling/samplings density was high at the site.

270

The substantial differences in CNS isotopic compositions in *A. marina* occurring between the two sites, suggested differences in the environmental conditions and biogeochemical processes that were possibly associated with the mangrove mortality effect. The leaf $\delta^{13}\text{C}$ values in the impacted forest were relatively enriched in ^{13}C . This C isotope pattern may be due to reduced stomatal conductance that causes lower internal carbon dioxide concentrations and lower carbon isotope fractionation
275 (Farquhar et al., 1989; Lin and Sternberg, 1992a; Lin and Sternberg, 1992b). Higher leaf $\delta^{13}\text{C}$ values can also be associated with increased carboxylation efficiency associated with higher nutrients, e.g. N in leaves (Cordell et al., 1999) and thicker leaves with higher internal resistance to carbon dioxide diffusion. Younger leaves can show higher $\delta^{13}\text{C}$ values than aged leaves due to ^{13}C enriched fractions (e.g. carbohydrates) transported from older autotrophic leaves to more heterotrophic young leaves (Werth et al., 2015). Leaves exposed to full sun can show higher $\delta^{13}\text{C}$ values than shaded leaves (Farquhar et al., 1989).

280 $\delta^{13}\text{C}$ values can also vary among different plant tissues in *A. marina* (Kelleway et al., 2018). Leaf N (%) did not differ between the two forests, suggesting that the two sites may have similar plant N availability. Previous studies show additions of nutrients such as N and/or P did not play a considerable role in mangrove leaf $\delta^{13}\text{C}$ variations (McKee et al., 2002), but salinity played an important role (Lin and Sternberg, 1992b). For example, leaf $\delta^{13}\text{C}$ values of *A. marina* at a lower salinity site was relatively depleted in ^{13}C and averaged about -31‰ (Kelleway et al., 2018). Overall, higher leaf $\delta^{13}\text{C}$ values in the impacted forest likely
285 suggest that there are chronic stresses associated with the dieback event that reduced stomatal conductance. Such environmental stresses may include hypersalinization of sediments and hydric, thermal and radiant stresses following canopy losses that cause higher evaporation and lower water availability. The leaves at the unimpacted site were largely depleted in

¹³C, suggesting that there was higher water availability at the unimpacted site, possibly associated with regional variability in groundwater flows, e.g., Sippo et al. 2020.

290

Leaf δ¹⁵N values varied more in the impacted (ranged from -0.9 to 6.7‰) than in the unimpacted forest (ranged from 2.9 to 6.2‰), but the means were similar ($4.3 \pm 1.9\text{‰}$ for the impacted and $4.4 \pm 0.8\text{‰}$ for the unimpacted), suggesting that two sites have similar background δ¹⁵N conditions. Generally, leaf δ¹⁵N varies due to N sources, microbial processes that enrich or deplete ¹⁵N in soil or water, and isotope fractionation during plant N uptake. Previous studies showed that in pristine mangrove forests, leaf δ¹⁵N values generally range around -2‰ to 3‰ (Fry and Smith, 2002; Smallwood et al., 2003). Such low δ¹⁵N values may reflect long-term N fixation inputs (e.g. around 0‰) (Fogel et al., 2008) and marine nitrate inputs (Dore et al., 2002). Much higher δ¹⁵N values (>10‰) may be associated with anthropogenic N inputs (Fry and Cormier, 2011). Our sites showed moderate δ¹⁵N values (about 4‰), suggesting that in addition to N fixation inputs and marine N inputs, there may be considerable microbial ¹⁵N enrichment in dissolved inorganic nitrogen pools of ammonium and nitrate. The higher variability in leaf δ¹⁵N in the impacted forest suggests higher variability in processes affecting the δ¹⁵N status of available N. For example, changes to sediment conditions including redox transitions and soil moisture content following the dieback may have affected microbial processes of N, whereas the unimpacted forest may have had more stable sediment conditions and N processes. Isotope fractionation during plant N uptake may also be an explanation for leaf δ¹⁵N variability (Fry et al., 2000), but such fractionation is poorly known for mangroves. A study reported that additions of P nutrients increased N demand and decreased δ¹⁵N fractionation (McKee et al., 2002), however as we did not measure P, we could not determine whether this was the case.

Leaf δ³⁴S values differed considerably between the two forests, with the impacted forest generally having higher values ($13.5 \pm 5.4\text{‰}$, range 7.7 to 23.3‰) than the unimpacted forest ($12.6 \pm 5.6\text{‰}$, range 5.0 to 21.9‰). Leaf δ³⁴S values showed trends along the six transects, with values decreasing from the upper to lower intertidal zones. Based on previous studies, mangrove leaf δ³⁴S values generally vary between -20 to 20‰ (Okada and Sasaki, 1995, 1998; Fry and Smith, 2002). Higher δ³⁴S values are likely associated with seawater sulfate, which is ³⁴S enriched (i.e. 21‰) and due to a large isotope fractionation (up to 70‰) during sulfate reduction (Kaplan and Rittenberg, 1964). Lower δ³⁴S values are likely associated with sedimentary sulfide-S that is ³⁴S depleted, for example, -21‰ (Okada and Sasaki, 1995). Leaf δ³⁴S values of around 14 to 18‰ suggest mangrove incorporations of seawater sulfate-S ($\delta^{34}\text{S}_{\text{S}} \sim 21\text{‰}$), with only a small isotopic fractionation occurring through absorption and assimilation steps (Okada and Sasaki, 1995). Plants generally show δ³⁴S values slightly lower than source sulfate-S by an average of -1.5‰ (Trust and Fry, 1992). Low leaf δ³⁴S values, for instance, the lowest value of 5‰ found in the unimpacted site suggest that the most probable source of this ³⁴S-depleted S is sulfide oxidation, followed by mixing with seawater sulfate. Low δ³⁴S values in mangrove root vascular tissues may indicate assimilation/oxidation of sulfide, potentially to reduce their toxic sulfide exposure (Fry et al., 1982; Raven et al., 2019), with reported isotope effect of -5.2‰ for non-biological oxidation of sulfide (Fry et al., 1988) and a smaller +1-3 ‰ effect for anaerobic oxidation of sulfide by

photosynthetic bacteria (Fry et al., 1984). An explanation for our observed $\delta^{34}\text{S}$ pattern may be lower plant incorporation of sulfide-S in the impacted site and also in the higher intertidal zones where we expect that mangrove sediment is relatively more oxidised, and the production of sulfide may be lower due to lower sulfate reduction.

4.2 Sediment

325 In healthy mangrove forests, the fate of C fixed by primary producers includes burial within the sediment, atmospheric emissions and outwelling to the ocean (Maher et al., 2018), but how mangrove mortality affects such processes is poorly understood. In most cases, C within in mangrove sediment decreases following forest loss due to degradation with increased CO₂ emissions (Otero et al., 2017; Adame et al., 2018). Lower TOC (%) and higher sediment $\delta^{13}\text{C}$ values in the impacted forest are probably related to sediment C loss and lower autochthonous C inputs (i.e. leaf litter) following the mangrove
330 mortality event. Consistent with this, the sediment N (%) and $\delta^{15}\text{N}$ data showed a similar pattern suggesting N loss and degradation. The surface sediment varied more than the subsurface fraction. This is probably because the surface fraction is generally more aerobic and remineralization of organic matter occurs more rapidly (Burdidge, 2011). Sediment $\delta^{13}\text{C}$ and ^{15}N values can increase during degradation of sediment organic matter following mangrove loss (Adame and Fry, 2016; Adame et al., 2018). Changes in sediment C and N may also be associated with root turnover. The MPB $\delta^{13}\text{C}$ values significantly differed,
335 with those from the impacted being higher than the unimpacted. The higher values probably indicate lower respiratory inputs of CO₂ from mangroves (Maher et al., 2013b). Our findings here are consistent with the finding of Sippo et al. (2019) that changes to oceanic carbon outwelling rates following mangrove loss are likely associated with a gradual loss of sediment carbon; similar to our finding of increased sediment $\delta^{13}\text{C}$ values in the impacted site, an isotope effect may have been due to loss of sediment mangrove C and/or replacement of mangrove peats with marine sediment.

340 4.3 Fauna

CNS isotopic compositions of consumers including an algae feeder, a grazer and a leaf feeder from the impacted site were more enriched in ^{13}C , ^{15}N and ^{34}S . These differences remained consistent throughout the three sampling of 2016, 2017 and 2018. Consistent with the findings from mangrove leaves, MPB and soil, the data suggested substantial changes in cycling of CNS associated with the mangrove mortality event. At the impacted site, consumers were more ^{13}C -enriched, likely due to the
345 loss of ^{13}C -depleted mangrove organic matter. Consumer $\delta^{13}\text{C}$ values can change due to changes to available organic matter, altered feeding dependencies as well as changes to organic matter $\delta^{13}\text{C}$ values. In our case, MPB $\delta^{13}\text{C}$ values changed significantly, likely due to changes to organic matter respiratory inputs and/or altered light environment and soil moisture contents that may change isotopic fractionation during carbon fixation. The consumer $\delta^{13}\text{C}$ values and their ranges at our study site are fairly consistent with the reported mangrove consumer $\delta^{13}\text{C}$ values elsewhere (e.g. Lee, 2000; Bouillon et al., 2002;
350 Demopoulos et al., 2007). The typical trophic enrichment factor for carbon isotope in small invertebrates is about +1‰ (Vander Zanden and Rasmussen, 2001; McCutchan et al., 2003). Lower consumer $\delta^{13}\text{C}$ values are generally associated with mangrove

detritus that is depleted in ^{13}C . Typical mangrove leaf-eating sesarmid crab species generally have tissue $\delta^{13}\text{C}$ values within about +5‰ from mangrove detritus (Bui and Lee, 2014). Higher $\delta^{13}\text{C}$ values of consumers are generally tied to MPB. Our MPB endmember $\delta^{13}\text{C}$ values of -25.2‰ for the unimpacted site and -21.5‰ for the impacted site did not match with the consumer $\delta^{13}\text{C}$ values (around -15 to -14‰), suggesting our characterization of MPB endmember $\delta^{13}\text{C}$ values was incomplete. This is probably because MPB can vary substantially within mangrove ecosystems (Bouillon et al., 2008) and consumers may be preferentially assimilating more ^{13}C enriched fractions of MPB, for example, diatom and/or filamentous cyanobacteria that can range about -15 to -20‰ (Craig, 1953; Fry and Wainright, 1991). The leaf feeders were relatively depleted in ^{13}C with $\delta^{13}\text{C}$ values of about -21 to -18‰, likely due to some use of mangrove leaves. Due to difficulties obtaining representative endmembers, mixing analysis was not achieved using this data to quantify feeding dependencies. However, MPB probably played an important dietary role in the both forests because the difference in MPB $\delta^{13}\text{C}$ values between the two forests were reflected in the difference in the consumers $\delta^{13}\text{C}$ values between the two forests (Harada et al. 2019).

Consistent with the mangrove leave $\delta^{34}\text{S}$ values, the consumer $\delta^{34}\text{S}$ values also indicated possible changes to S cycling. The consumer $\delta^{34}\text{S}$ values were generally higher in the impacted site (range 13.4 to 21.7‰) than in the unimpacted site (range 8.2 to 16‰) suggesting lower sulfate reduction with decreased sulfide inputs at the impacted site. Fixation of sulfate by phytoplankton occurs with a small isotope effect, around 1 to 2‰ (Fry, 2006), therefore phytoplankton $\delta^{34}\text{S}$ values from the coastal ocean are generally close to the seawater sulfate-S value of 21‰. MPB generally have lower $\delta^{34}\text{S}$ values than phytoplankton, e.g. near 10‰ for MPB in a mangrove ecosystem (Harada et al., unpublished), likely due to some use of sedimentary sulfide-S (depleted in ^{34}S). Our consumer $\delta^{34}\text{S}$ values were lower than 21‰, suggesting some use of MPB as well as mangrove detritus. The consumer $\delta^{15}\text{N}$ also indicates possible changes to N cycling, with the consumer in the impacted site generally having higher values than those from in the unimpacted site. The higher $\delta^{15}\text{N}$ values are likely associated with degradation of organic matter, microbial ^{15}N enrichment in dissolved inorganic N during degradation and lower N fixation inputs that typically show low $\delta^{15}\text{N}$ values. While the $\delta^{13}\text{C}$ and $\delta^{34}\text{S}$ values consistently differed between the two forests during the two-year survey, the $\delta^{15}\text{N}$ values started showing matches between the two forests in 2018, likely suggesting recovery of $\delta^{15}\text{N}$ status to the background conditions, and/or that the recovery of N may be faster than C and S elements. This may be the case as mangrove ecosystems are generally N limited (Reef et al., 2010), and circulation of N elements is faster than those of C and S elements.

4.4 Compound-specific isotope analysis of amino acids

It is considered that environmental resources such as vascular plants and microalgae have a different $\delta^{13}\text{C}$ pattern ('fingerprint') in AAs due to differing biosynthesis of AAs (Larsen et al., 2009; Larsen et al., 2013). It is also reported that $\delta^{13}\text{C}$ patterns are largely unaffected by environmental conditions. For example, $\delta^{13}\text{C}_{\text{AA}}$ patterns of the marine diatom *Thalassiosira weissflogii*

did not respond to changing environmental conditions such as light, salinity, temperature and pH, despite substantial changes in bulk $\delta^{13}\text{C}$ values (Larsen et al., 2015). A similar isotope pattern was reported for seagrass *Posidonia oceanica* and the giant kelp *Macrocystis pyrifera*, which showed consistent $\delta^{13}\text{C}_{\text{AA}}$ patterns despite varying season and growth conditions (Larsen et al., 2013). The $\delta^{13}\text{C}_{\text{AA}}$ patterns in producers, especially those of essential amino acids ($\delta^{13}\text{C}_{\text{EAA}}$), can be reflected in consumer tissues with little isotope effect. This is because animals obtain EAAs from their diet and EAA fractions are thought to be directly assimilated (McMahon et al., 2010). These general expectations were reasonably met in our $\delta^{13}\text{C}_{\text{EAA}}$ dataset. Normalized $\delta^{13}\text{C}_{\text{EAA}}$ patterns of our producer samples including mangrove leaves (yellow leaves of *A. marina*) and MPB did not differ between the two sites despite differing environmental conditions and substantial differences in bulk $\delta^{13}\text{C}$ values (Table 4, Fig 6 and Fig S1). Furthermore, the consumer $\delta^{13}\text{C}_{\text{EAA}}$ patterns also did not differ between the two sites. (Fig. 6 and Fig S1). These findings did not support changes to feeding dependency following mangrove loss but suggested that the overall differences in the consumer bulk $\delta^{13}\text{C}$ values were most likely driven by differences in the resource organic matter $\delta^{13}\text{C}$ values e.g. changes to MPB $\delta^{13}\text{C}$ values that were likely associated with lower mangrove C fixation/respiratory inputs following the mangrove mortality. Furthermore, such findings indicate that the reported substantial change to the mangrove benthic faunal assemblage following the mangrove loss (Harada et al., 2019) was probably driven more by modification of physical habitat structure than changes in the use of food resources.

5 Conclusions

Reporting rare and extreme biological events can be complicated because in many cases they may occur suddenly, therefore drawing comparisons between pre and post event conditions remains a challenge. Our field investigations using traditional ecological techniques combined with SIA measured the initial dieback and also early recovery of an impacted mangrove ecosystem and compared an adjacent unimpacted reference system. Although the unimpacted and impacted forests were not replicated in this study, the difference between the two sites was clear. Mangrove seedling and sapling populations that increased during the period from 2016 to 2018 (8 to 32 months after the mortality event) in the impacted site, suggest recovery of the mangrove vegetation. This also suggests that the environmental conditions at the impacted site are still conducive for re-establishment of mangroves, allowing recruitment of seedlings and development of regrowth. However, mangrove leaves collected in the impacted site in 2018 showed relatively higher $\delta^{13}\text{C}$ values ($-25.8 \pm 1.0\text{\textperthousand}$) that are probably associated with continued water stress. Invertebrates from the impacted site representing the feeding types of grazing, leaf feeding, and algae feeding were more enriched in ^{13}C , ^{15}N and ^{34}S relative to those from the unimpacted site. For example, they were more ^{13}C enriched at the impacted site, by $1.7 - 4.1\text{\textperthousand}$ and the difference did not change over the study period. Overall, our stable CNS isotope data supported the hypothesis that changes to biogeochemical processes occur following the mangrove mortality. These changes include lower mangrove C fixation/respiration, lower N fixation and lower sulfate reduction. However, our isotope data did not support the second hypothesis that the isotopic compositions change over time with recovery of mangrove

vegetation. Recovery of biogeochemical processes was not evident even after two years, suggesting an ongoing impact of the
415 mortality event. An exception was that N cycle recovery may be occurring faster.

Considering that the environmental conditions at the site play an important role in facilitating recolonisation of mangroves, we conceptualise the recovery of the mangrove forest under four different scenarios to give insight into the ecological and biogeochemical consequences of changing forest conditions (Fig. 7): 1) The forest recovers with mangroves being able to
420 recolonise at the site without future perturbations; 2) the forest recovers with future perturbations such as climatic events, for example, mangrove recolonisation is driven by events as such ENSO cycles; 3) the forest does not recover and is transformed into intertidal mudflats; and 4) the forest recovers partially at the site and in a reduced size and/or is recolonised by other plants such as saltmarshes, e.g., mangroves only recolonise in the lower intertidal zone. Each of these scenarios will have a distinct isotopic trajectory for C, N and S. While these are likely scenarios and there might be other possibilities, comparing the
425 impacted forest and an adjacent unimpacted reference forest can help us quantify the recovery. Continued monitoring of the post-dieback forest would be required to predict the long-term trajectory of ecosystem recovery and how on-going climate change and extreme climatic events affect the recovery of mangroves in the impacted region. In such a long-term investigation, SIA is a powerful tool, capable of tracking changes in biogeochemical processes over time. As such, it is of great assistance in ecosystem analyses and detecting the underlying biological mechanisms that drive changes and recovery.

430

Author contributions. The study was conceptualized by all authors. Writing was led by YH and contributed to by all. Field surveys were executed by DTM, JZS, LCJ, AJB and YH. Data compilation and analysis was coordinated by YH and contributed to by all.

435 *Competing interests.* The authors declare no competing interests.

Acknowledgments. We acknowledge support from: YH – Holsworth Wildlife Research Endowment – Equity Trustees Charitable Foundation & the Ecological Society of Australia; DTM - Australian Research Council (DE1500100581, DP180101285); RMC – Global Wetlands Project. We thank R. Bak and V. Fry (Griffith University) for stable isotope analysis.

440 Field work was assisted by G. Reithmaier, K. Maguire, D. Brown, S. Conrad, A. McMahon, C. Holloway, M. Call, A. Gauthey, G. Balland and J. Kalla. M. Hayes commented on and improved early versions of the manuscript.

References

- Abrantes, K. G., Johnston, R., Connolly, R. M., and Sheaves, M.: Importance of Mangrove Carbon for Aquatic Food Webs in
445 Wet–Dry Tropical Estuaries, *Estuaries and Coasts*, 38, 383-399, 2015.
- Adame, M., and Fry, B.: Source and stability of soil carbon in mangrove and freshwater wetlands of the Mexican Pacific coast,
Wetlands ecology and management, 24, 129-137, 2016.
- Adame, M., Zakaria, R., Fry, B., Chong, V., Then, Y., Brown, C., and Lee, S. Y.: Loss and recovery of carbon and nitrogen
after mangrove clearing, *Ocean & Coastal Management*, 161, 117-126, 2018.
- 450 Asbridge, E., Lucas, R., Ticehurst, C., and Bunting, P.: Mangrove response to environmental change in Australia's Gulf of
Carpentaria, *Ecology and Evolution*, 6, 3523-3539, 2016.
- Asbridge, E., Lucas, R., Rogers, K., and Accad, A.: The extent of mangrove change and potential for recovery following severe
Tropical Cyclone Yasi, Hinchinbrook Island, Queensland, Australia, *Ecology and evolution*, 8, 10416-10434, 2018.
- 455 Asbridge, E. F., Bartolo, R., Finlayson, C. M., Lucas, R. M., Rogers, K., and Woodroffe, C. D.: Assessing the distribution and
drivers of mangrove dieback in Kakadu National Park, northern Australia, *Estuarine, Coastal and Shelf Science*, 106353, 2019.
- Bernardino, A. F., Gomes, L. E. D. O., Hadlich, H. L., Andrades, R., and Correa, L. B.: Mangrove clearing impacts on
macrofaunal assemblages and benthic food webs in a tropical estuary, *Marine Pollution Bulletin*, 126, 228-235, 2018.
- Bouillon, S., Koedam, N., Raman, A., and Dehairs, F.: Primary producers sustaining macro-invertebrate communities in
intertidal mangrove forests, *Oecologia*, 130, 441-448, 2002.
- 460 Bouillon, S., Connolly, R. M., and Lee, S. Y.: Organic matter exchange and cycling in mangrove ecosystems: Recent insights
from stable isotope studies, *Journal of Sea Research*, 59, 44-58, 2008.
- Bui, T. H. H., and Lee, S. Y.: Does ‘You Are What You Eat’ Apply to Mangrove Grapsid Crabs?, *PLOS ONE*, 9, e89074,
2014.
- Burdige, D.: 5.09 Estuarine and coastal sediments–coupled biogeochemical cycling, *Treatise on Estuarine and Coastal Science*,
465 5, 279-308, 2011.
- Cahoon, D. R., Hensel, P., Rybczyk, J., McKee, K. L., Proffitt, C. E., and Perez, B. C.: Mass tree mortality leads to mangrove
peat collapse at Bay Islands, Honduras after Hurricane Mitch, *Journal of Ecology*, 91, 1093-1105, 2003.
- Connolly, R. M., Connolly, F. N., Hayes, M. A.: Oil spill from the Era: Mangroves taking eons to recover, *Marine Pollution
Bulletin*, 153, 110965, 2020.
- 470 Cordell, S., Goldstein, G., Meinzer, F. C., and Handley, L. L.: Allocation of nitrogen and carbon in leaves of *Metrosideros
polymorpha* regulates carboxylation capacity and $\delta^{13}\text{C}$ along an altitudinal gradient, *Functional Ecology*, 13, 811-818, 1999.
- Coumou, D., and Rahmstorf, S.: A decade of weather extremes, *Nature Climate Change*, 2, 491-496, 2012.
- Craig, H.: The geochemistry of the stable carbon isotopes, *Geochimica et Cosmochimica Acta*, 3, 53-92, 1953.
- Demopoulos, A. W., Fry, B., and Smith, C. R.: Food web structure in exotic and native mangroves: a Hawaii–Puerto Rico
475 comparison, *Oecologia*, 153, 675-686, 2007.

- Docherty, G., Jones, V., and Evershed, R. P.: Practical and theoretical considerations in the gas chromatography/combustion/isotope ratio mass spectrometry $\delta^{13}\text{C}$ analysis of small polyfunctional compounds, *Rapid Communications in Mass Spectrometry*, 15, 730-738, 2001.
- 480 Dore, J. E., Brum, J. R., Tupas, L. M., and Karl, D. M.: Seasonal and interannual variability in sources of nitrogen supporting export in the oligotrophic subtropical North Pacific Ocean, *Limnology and Oceanography*, 47, 1595-1607, 2002.
- Duke, N. C., Kovacs, J. M., Griffiths, A. D., Preece, L., Hill, D. J., Van Oosterzee, P., Mackenzie, J., Morning, H. S., and Burrows, D.: Large-scale dieback of mangroves in Australia's Gulf of Carpentaria: a severe ecosystem response, coincidental with an unusually extreme weather event, *Marine and Freshwater Research*, 68, 1816-1829, 2017.
- 485 Farquhar, G. D., Ehleringer, J. R., and Hubick, K. T.: Carbon isotope discrimination and photosynthesis, *Annual review of plant biology*, 40, 503-537, 1989.
- Fogel, M., Wooller, M., Cheeseman, J., Smallwood, B., Roberts, Q., Romero, I., and Meyers, M. J.: Unusually negative nitrogen isotopic compositions ($\delta^{15}\text{N}$) of mangroves and lichens in an oligotrophic, microbially-influenced ecosystem, *Biogeosciences*, 5, 1693-1704, 2008.
- 490 Fry, B., Scalan, R. S., Winters, J. K., and Parker, P. L.: Sulphur uptake by salt grasses, mangroves, and seagrasses in anaerobic sediments, *Geochimica et Cosmochimica Acta*, 46, 1121-1124, 1982.
- Fry, B., Gest, H., and Hayes, J. M.: Isotope effects associated with the anaerobic oxidation of sulfide by the purple photosynthetic bacterium, *Chromatium vinosum*, *FEMS Microbiology Letters*, 22, 283-287, 1984.
- Fry, B., Ruf, W., Gest, H., and Hayes, J. M.: Sulfur isotope effects associated with oxidation of sulfide by O_2 in aqueous solution, *Chemical Geology: Isotope Geoscience section*, 73, 205-210, 1988.
- 495 Fry, B., and Wainright, S. C.: Diatom sources of ^{13}C -rich carbon in marine food webs, *Marine Ecology Progress Series*, 149-157, 1991.
- Fry, B., Bern, A. L., Ross, M. S., and Meeder, J. F.: $\delta^{15}\text{N}$ Studies of Nitrogen Use by the Red Mangrove, *Rhizophora mangle* L. in South Florida, *Estuarine, Coastal and Shelf Science*, 50, 291-296, 2000.
- 500 Fry, B., and Smith, T. J.: Stable isotope studies of red mangroves and filter feeders from the Shark River estuary, Florida, *Bulletin of Marine Science*, 70, 871-890, 2002.
- Fry, B.: Stable isotope ecology, Springer, 2006.
- Fry, B., and Cormier, N.: Chemical Ecology of Red Mangroves, *Rhizophora mangle*, in the Hawaiian Islands1, *Pacific Science*, 65, 219-235, 2011.
- Harada, Y., Fry, B., Lee, S. Y., Maher, D. T., Sippo, J. Z., and Connolly, R. M.: Stable isotopes indicate ecosystem restructuring following climate-driven mangrove dieback, *Limnology and Oceanography*, 2019.
- 505 Harada, Y., and Lee, S. Y.: Foraging behavior of the mangrove sesarmid crab *Neosarmatium trispinosum* enhances food intake and nutrient retention in a low-quality food environment, *Estuarine, Coastal and Shelf Science*, 174, 41-48, 2016.
- Harris, R. M. B., Beaumont, L. J., Vance, T. R., Tozer, C. R., Remenyi, T. A., Perkins-Kirkpatrick, S. E., Mitchell, P. J., Nicotra, A. B., McGregor, S., Andrew, N. R., Letnic, M., Kearney, M. R., Wernberg, T., Hutley, L. B., Chambers, L. E.,

- 510 Fletcher, M. S., Keatley, M. R., Woodward, C. A., Williamson, G., Duke, N. C., and Bowman, D. M. J. S.: Biological responses to the press and pulse of climate trends and extreme events, *Nature Climate Change*, 8, 579-587, 2018.
- Harris, T., Hope, P., Oliver, E., Smalley, R., Arblaster, J., Holbrook, N., Duke, N., Pearce, K., Braganza, K., and Bindoff, N.: Climate drivers of the 2015 Gulf of Carpentaria mangrove dieback, *Earth Systems and Climate Change Hub Technical Report No, 2*, 2017.
- 515 Hayes, M. A., Jesse, A., Welti, N., Tabet, B., Lockington, D., and Lovelock, C. E.: Groundwater enhances above-ground growth in mangroves, *Journal of Ecology*, 107, 1120-1128, 2019.
- Hughes, T. P., Kerry, J. T., Álvarez-Noriega, M., Álvarez-Romero, J. G., Anderson, K. D., Baird, A. H., Babcock, R. C., Beger, M., Bellwood, D. R., Berkelmans, R., Bridge, T. C., Butler, I. R., Byrne, M., Cantin, N. E., Comeau, S., Connolly, S. R., Cumming, G. S., Dalton, S. J., Diaz-Pulido, G., Eakin, C. M., Figueira, W. F., Gilmour, J. P., Harrison, H. B., Heron, S. F., Hoey, A. S., Hobbs, J. P. A., Hoogenboom, M. O., Kennedy, E. V., Kuo, C. Y., Lough, J. M., Lowe, R. J., Liu, G., McCulloch, M. T., Malcolm, H. A., McWilliam, M. J., Pandolfi, J. M., Pears, R. J., Pratchett, M. S., Schoepf, V., Simpson, T., Skirving, W. J., Sommer, B., Torda, G., Wachenfeld, D. R., Willis, B. L., and Wilson, S. K.: Global warming and recurrent mass bleaching of corals, *Nature*, 543, 373-377, 2017.
- 520 Imbert, D., Rousteau, A., and Scherrer, P.: Ecology of mangrove growth and recovery in the Lesser Antilles: state of knowledge and basis for restoration projects, *Restoration Ecology*, 8, 230-236, 2000.
- Ishikawa, N. F., Chikaraishi, Y., Takano, Y., Sasaki, Y., Takizawa, Y., Tsuchiya, M., Tayasu, I., Nagata, T., and Ohkouchi, N.: A new analytical method for determination of the nitrogen isotopic composition of methionine: Its application to aquatic ecosystems with mixed resources, *Limnology and Oceanography: Methods*, 16, 607-620, 2018.
- Jeffrey, L.C., Reithmaier, G., Sippo, J.Z., Johnston, S.G., Tait, D.R., Harada, Y. and Maher, D.T. : Are methane emissions from mangrove stems a cryptic carbon loss pathway? Insights from a catastrophic forest mortality, *New Phytol*, 224, 146-154, 2019.
- Kaplan, I., and Rittenberg, S.: Microbiological fractionation of sulphur isotopes, *Microbiology*, 34, 195-212, 1964.
- Kelleway, J. J., Mazumder, D., Baldock, J. A., and Saintilan, N.: Carbon isotope fractionation in the mangrove Avicennia marina has implications for food web and blue carbon research, *Estuarine, Coastal and Shelf Science*, 205, 68-74, 2018.
- 535 Krauss, K. W., and Osland, M. J.: Tropical cyclones and the organization of mangrove forests: a review, *Annals of Botany*, 2019.
- Larsen, T., Taylor, D. L., Leigh, M. B., and O'Brien, D. M.: Stable isotope fingerprinting: a novel method for identifying plant, fungal, or bacterial origins of amino acids, *Ecology*, 90, 3526-3535, 2009.
- Larsen, T., Wooller, M. J., Fogel, M. L., and O'Brien, D. M.: Can amino acid carbon isotope ratios distinguish primary producers in a mangrove ecosystem?, *Rapid Communications in Mass Spectrometry*, 26, 1541-1548, 2012.
- 540 Larsen, T., Ventura, M., Andersen, N., O'Brien, D. M., Piatkowski, U., and McCarthy, M. D.: Tracing Carbon Sources through Aquatic and Terrestrial Food Webs Using Amino Acid Stable Isotope Fingerprinting, *PLoS ONE*, 8, e73441, 2013.

- Larsen, T., Bach, L. T., Salvatteci, R., Wang, Y. V., Andersen, N., Ventura, M., and McCarthy, M. D.: Assessing the potential of amino acid ^{13}C patterns as a carbon source tracer in marine sediments: effects of algal growth conditions and sedimentary diagenesis, *Biogeosciences*, 12, 4979-4992, 2015.
- Lee, S. Y.: Carbon dynamics of Deep Bay, eastern Pearl River estuary, China. II: Trophic relationship based on carbon-and nitrogen-stable isotopes, *Marine Ecology Progress Series*, 205, 1-10, 2000.
- Lin, G., and Sternberg, L.: Differences in morphology, carbon isotope ratios, and photosynthesis between scrub and fringe mangroves in Florida, USA, *Aquatic Botany*, 42, 303-313, 1992a.
- 545 Lin, G., and Sternberg, L.: Effect of growth form, salinity, nutrient and sulfide on photosynthesis, carbon isotope discrimination and growth of red mangrove (*Rhizophora mangle* L.), *Functional Plant Biology*, 19, 509-517, 1992b.
- Lovelock, C. E., Feller, I. C., Reef, R., Hickey, S., and Ball, M. C.: Mangrove dieback during fluctuating sea levels, *Scientific Reports*, 7, 1680, 2017.
- Maher, D. T., Santos, I. R., Golsby-Smith, L., Gleeson, J., and Eyre, B. D.: Groundwater-derived dissolved inorganic and 555 organic carbon exports from a mangrove tidal creek: The missing mangrove carbon sink?, *Limnology and Oceanography*, 58, 475-488, 2013a.
- Maher, D. T., Santos, I. R., Leuven, J. R. F. W., Oakes, J. M., Erler, D. V., Carvalho, M. C., and Eyre, B. D.: Novel Use of Cavity Ring-down Spectroscopy to Investigate Aquatic Carbon Cycling from Microbial to Ecosystem Scales, *Environmental Science & Technology*, 47, 12938-12945, 2013b.
- 560 Maher, D. T., Santos, I. R., Schulz, K. G., Call, M., Jacobsen, G. E., and Sanders, C. J.: Blue carbon oxidation revealed by radiogenic and stable isotopes in a mangrove system, *Geophysical Research Letters*, 44, 4889-4896, 2017.
- Maher, D. T., Call, M., Santos, I. R., and Sanders, C. J.: Beyond burial: lateral exchange is a significant atmospheric carbon sink in mangrove forests, *Biology Letters*, 14, 20180200, 2018.
- Mbense, S., Rajkaran, A., Bolosha, U., and Adams, J.: Rapid colonization of degraded mangrove habitat by succulent salt 565 marsh, *South African journal of botany*, 107, 129-136, 2016.
- McCutchan, J. H., Lewis Jr, W. M., Kendall, C., and McGrath, C. C.: Variation in trophic shift for stable isotope ratios of carbon, nitrogen, and sulfur, *Oikos*, 102, 378-390, 2003.
- McKee, K. L., Feller, I. C., Popp, M., and Wanek, W.: Mangrove isotopic ($\delta^{15}\text{N}$ and $\delta^{13}\text{C}$) fractionation across a nitrogen vs. phosphorus limitation gradient, *Ecology*, 83, 1065-1075, 2002.
- 570 McKee, K. L., Rooth, J. E., and Feller, I. C.: Mangrove recruitment after forest disturbance is facilitated by herbaceous species in the Caribbean, *Ecological Applications*, 17, 1678-1693, 2007.
- McMahon, K. W., Fogel, M. L., Elsdon, T. S., and Thorrold, S. R.: Carbon isotope fractionation of amino acids in fish muscle reflects biosynthesis and isotopic routing from dietary protein, *Journal of Animal Ecology*, 79, 1132-1141, 2010.
- Milbrandt, E., Greenawalt-Boswell, J., Sokoloff, P., and Bortone, S.: Impact and response of Southwest Florida mangroves to 575 the 2004 hurricane season, *Estuaries and Coasts*, 29, 979-984, 2006.

Ohkouchi, N., Chikaraishi, Y., Close, H. G., Fry, B., Larsen, T., Madigan, D. J., McCarthy, M. D., McMahon, K. W., Nagata, T., Naito, Y. I., Ogawa, N. O., Popp, B. N., Steffan, S., Takano, Y., Tayasu, I., Wyatt, A. S. J., Yamaguchi, Y. T., and Yokoyama, Y.: Advances in the application of amino acid nitrogen isotopic analysis in ecological and biogeochemical studies, *Organic Geochemistry*, 113, 150-174, 2017.

- 580 Okada, N., and Sasaki, A.: Characteristics of Sulfur Uptake by Mangroves: an Isotopic Study, *Tropics*, 4, 201-210, 1995.
Okada, N., and Sasaki, A.: Sulfur isotopic composition of mangroves, *Isotopes in environmental and health studies*, 34, 61-65, 1998.
- Otero, X. L., Méndez, A., Nóbrega, G. N., Ferreira, T. O., Santiso-Taboada, M. J., Meléndez, W., and Macías, F.: High fragility of the soil organic C pools in mangrove forests, *Marine Pollution Bulletin*, 119, 460-464, 2017.
- 585 Rashid, S., Biswas, S. R., Böcker, R., and Kruse, M.: Mangrove community recovery potential after catastrophic disturbances in Bangladesh, *Forest Ecology and Management*, 257, 923-930, 2009.
- Raven, M. R., Fike, D. A., Gomes, M. L., and Webb, S. M.: Chemical and isotopic evidence for organic matter sulfurization in redox gradients around mangrove roots, *Frontiers in Earth Science*, 7, 98, 2019.
- Reef, R., Feller, I. C., and Lovelock, C. E.: Nutrition of mangroves, *Tree Physiology*, 30, 1148-1160, 2010.
- 590 Riekenberg, P. M., Carney, R. S., and Fry, B.: Trophic plasticity of the methanotrophic mussel *Bathymodiolus childressi* in the Gulf of Mexico, *Marine Ecology Progress Series*, 547, 91-106, 2016.
- Santini, N. S., Reef, R., Lockington, D. A., and Lovelock, C. E.: The use of fresh and saline water sources by the mangrove *Avicennia marina*, *Hydrobiologia*, 745, 59-68, 2015.
- Sasmito, S. D., Kuzyakov, Y., Lubis, A. A., Murdiyarso, D., Hutley, L. B., Bachri, S., Friess, D. A., Martius, C., Borchard, 595 N.: Organic carbon burial and sources in soils of coastal mudflat and mangrove ecosystems, *CATENA*, 187, 104414, 2020.
- Sherman, R. E., Fahey, T. J., and Martinez, P.: Hurricane Impacts on a Mangrove Forest in the Dominican Republic: Damage Patterns and Early Recovery 1, *Biotropica*, 33, 393-408, 2001.
- Silliman, B. R., van de Koppel, J., Bertness, M. D., Stanton, L. E., and Mendelssohn, I. A.: Drought, Snails, and Large-Scale Die-Off of Southern U.S. Salt Marshes, *Science*, 310, 1803-1806, 2005.
- 600 Sippo, J. Z., Lovelock, C. E., Santos, I. R., Sanders, C. J., and Maher, D. T.: Mangrove mortality in a changing climate: An overview, *Estuarine, Coastal and Shelf Science*, 215, 241-249, 2018.
- Sippo, J. Z., Maher, D. T., Schulz, K. G., Sanders, C. J., McMahon, A., Tucker, J., and Santos, I. R.: Carbon outwelling across the shelf following a massive mangrove dieback in Australia: Insights from radium isotopes, *Geochimica et Cosmochimica Acta*, 253, 142-158, 2019.
- 605 Sippo, J. Z., Sanders, C. J., Santos, I. R., Jeffrey, L. C., Call, M., Harada, Y., Maguire, K., Brown, D., Conrad, S. R. and Maher, D.T.: Coastal carbon cycle changes following mangrove loss. *Limnology and Oceanography*, 2020b.
- Sippo, J. Z., Santos, I. R., Sanders, C. J., Gadd, P., Hua, Q., Lovelock, C. E., Santini, N. S., Johnston S. G., Harada, Y., Reithmeir, G., and Maher, D. T.: Reconstructing extreme climatic and geochemical conditions during the largest natural mangrove dieback on record, *Biogeosciences*, 2020a.

- 610 Sjöling, S., Mohammed, S. M., Lyimo, T. J., and Kyaruzi, J. J.: Benthic bacterial diversity and nutrient processes in mangroves: impact of deforestation, *Estuarine, Coastal and Shelf Science*, 63, 397-406, 2005.
- Smallwood, B. J., Wooller, M. J., Jacobson, M. E., and Fogel, M. L.: Isotopic and molecular distributions of biochemicals from fresh and buried *Rhizophora* mangle leaves, *Geochemical Transactions*, 4, 38, 2003.
- Smith, T. J., Robblee, M. B., Wanless, H. R., and Doyle, T. W.: Mangroves, hurricanes, and lightning strikes: assessment of
615 Hurricane Andrew suggests an interaction across two differing scales of disturbance, *BioScience*, 44, 256-262, 1994.
- Stott, P.: How climate change affects extreme weather events, *Science*, 352, 1517-1518, 2016.
- Sweetman, A., Middelburg, J., Berle, A., Bernardino, A., Schander, C., Demopoulos, A., and Smith, C.: Impacts of exotic mangrove forests and mangrove deforestation on carbon remineralization and ecosystem functioning in marine sediments, *Biogeosciences*, 7, 2129-2145, 2010.
- 620 Thomson, J. A., Burkholder, D. A., Heithaus, M. R., Fourqurean, J. W., Fraser, M. W., Statton, J., and Kendrick, G. A.: Extreme temperatures, foundation species, and abrupt ecosystem change: an example from an iconic seagrass ecosystem, *Global Change Biology*, 21, 1463-1474, 2015.
- Tomlinson, P. B.: *The botany of mangroves*, Cambridge University Press, 2016.
- Trust, B., and Fry, B.: Stable sulphur isotopes in plants: a review, *Plant, Cell & Environment*, 15, 1105-1110, 1992.
- 625 Vander Zanden, M. J., and Rasmussen, J. B.: Variation in $\delta^{15}\text{N}$ and $\delta^{13}\text{C}$ trophic fractionation: Implications for aquatic food web studies, *Limnology and Oceanography*, 46, 2061-2066, 2001.
- Wernberg, T., Bennett, S., Babcock, R. C., de Bettignies, T., Cure, K., Depczynski, M., Dufois, F., Fromont, J., Fulton, C. J., Hovey, R. K., Harvey, E. S., Holmes, T. H., Kendrick, G. A., Radford, B., Santana-Garcon, J., Saunders, B. J., Smale, D. A., Thomsen, M. S., Tuckett, C. A., Tuya, F., Vanderklift, M. A., and Wilson, S.: Climate-driven regime shift of a temperate
630 marine ecosystem, *Science*, 353, 169-172, 2016.
- Werth, M., Mehltreter, K., Briones, O., and Kazda, M.: Stable carbon and nitrogen isotope compositions change with leaf age in two mangrove ferns, *Flora-Morphology, Distribution, Functional Ecology of Plants*, 210, 80-86, 2015.

635 **Table 1.** Spatial and temporal details of the sampling design (x = sampled).

	Sampling plots along each transect					Year			
	Forest edge, landward	High	Mid	Low	Forest edge, seaward	Mudflat	2016, 8 months after dieback	2017, 20 months after dieback	2018, 32 months after dieback
Mangrove seedling count		x					x	x	x
Bulk SIA invertebrates*		x	x	x			x	x	x
CSIA invertebrates*		x	x	x				x	
Bulk SIA mangrove leaves	x	x	x	x	x				x
Bulk SIA mangrove wood			x						x
Bulk SIA surface sediment	x	x	x	x	x	x			x
Bulk SIA subsurface sediment			x						x

*for invertebrate SIA, to gain sufficient sampling size, high, mid and low plots were pooled for analysis.

640 **Table 2.** Elemental and isotopic compositions of the mangrove *A. marina* (mean, SD) in 2018, 32 months after the dieback.

Tissue type	Forest	%C	%N	%S	$\delta^{13}\text{C}$, ‰	$\delta^{15}\text{N}$, ‰	$\delta^{34}\text{S}$, ‰	n
Green leaf	Unimpacted	39.3 ± 1.7	1.75 ± 0.37	0.54 ± 0.23	-28.4 ± 1.5	4.4 ± 0.8	12.6 ± 5.6	15
	Impacted	40.0 ± 1.6	1.82 ± 0.45	0.73 ± 0.14	-25.8 ± 1.0	4.3 ± 1.9	13.5 ± 5.4	15
Yellow leaf	Unimpacted	41.6 ± 2.2	0.67 ± 0.23	1.18 ± 0.47	-26.4 ± 1.3	6.5 ± 1.1	14.6 ± 7.7	3
	Impacted	41.9 ± 1.0	0.52 ± 0.05	1.18 ± 0.38	-26.2 ± 0.6	7.4 ± 0.2	12.5 ± 2.8	3
Wood	Unimpacted	42.6 ± 3.0	0.38 ± 0.27	0.04 ± 0.01	-24.8 ± 1.8	6.1 ± 2.0	-	2
	Impacted	39.9 ± 5.7	0.40 ± 0.16	0.31 ± 0.37	-24.9 ± 1.0	4.7 ± 1.0	-	2

Table 3. Elemental and isotopic compositions of sediment in 2018, 32 months after the dieback (mean, SD).

	Forest/site	% TOC	% TN	C:N	$\delta^{13}\text{C}$, ‰	$\delta^{15}\text{N}$, ‰	n
Mangrove forest, 0 to 0.5 cm	Unimpacted	2.02 ± 1.16	0.15 ± 0.06	13.48 ± 2.49	-24.3 ± 1.2	2.0 ± 0.5*	15
	Impacted	1.06 ± 0.37	0.09 ± 0.03	11.67 ± 2.58	-21.8 ± 1.0	2.8 ± 0.6*	15
Mangrove forest, 0.5 to 20 cm	Unimpacted	1.83 ± 0.73	0.12 ± 0.04	15.12 ± 1.79	-25.2 ± 0.9	1.7 ± 0.5*	6
	Impacted	1.29 ± 0.55	0.09 ± 0.03	14.71 ± 2.81	-24.4 ± 0.5	1.7 ± 0.3*	6
Mudflat, 0 to 0.5 cm	Unimpacted	1.02 ± 0.08	0.11 ± 0.01	9.07 ± 0.91	-21.8 ± 0.8	-	3
	Impacted	0.58 ± 0.18	0.07 ± 0.02	8.78 ± 0.93	-21.2 ± 0.9	-	3
Saltpan, 0 to 0.5 cm	Unimpacted	1.87 ± 2.03	0.19 ± 0.24	11.44 ± 3.05	-18.9 ± 1.7	-	4
	Impacted	0.83 ± 0.07	0.07 ± 0.01	11.82 ± 0.69	-20.8 ± 0.7	-	4
Offshore, 0 to 0.5 cm	1km offshore	0.77 ± 0.28	0.08 ± 0.03	11.89 ± 8.31	-21.5 ± 1.1	-	5
POM	1km offshore	-	-	-	-21.1 ± 1.5	3.6 ± 2.1	3
MPB	Unimpacted	-	-	-	-25.2 ± 1.0	-	6
	Impacted	-	-	-	-21.5 ± 1.3	-	6

*values were taken from Harada et al. (2019)

645 **Table 4.** Bulk $\delta^{13}\text{C}$ values, mean $\delta^{13}\text{C}$ values of five EAAs (‰) and differences (Δ , ‰) between the two forests in 2017, 20 months after the dieback (mean \pm SD).

Group	Taxa	Forest	Bulk $\delta^{13}\text{C}$,	Mean $\delta^{13}\text{C}$	n	Δ Bulk	Δ Mean $\delta^{13}\text{C}$	Permano
			‰	of five EAAs, ‰		$\delta^{13}\text{C}$, ‰	of five EAAs, ‰	va
						%		p value
Algal feeder	<i>Tubuca</i> <i>signata</i>	Unimpacted Impacted	-17.1 \pm 1.4 -15.4 \pm 1.4	-21.9 \pm 1.5 -20.5 \pm 1.8	3	1.7	1.4	0.90
Leaf feeder	<i>Parasesarma</i> <i>/ Episesarma</i>	Unimpacted Impacted	-21.4 \pm 1.5 -18.3 \pm 0.2	-25.3 \pm 1.6 -23.9 \pm 0.1	3	3.1	1.4	0.40
Grazer	<i>Telescopium</i> <i>telescopium</i>	Unimpacted Impacted	-18.2 \pm 1.9 -16.7 \pm 1.3	-24.0 \pm 1.8 -22.2 \pm 1.1	3	1.5	1.8	0.80
Filter feeder	<i>Crassostrea</i> (oyster)	Unimpacted Impacted	-19.3 \pm 0.4 -19.0 \pm 0.8	-22.8 \pm 0.2 -22.9 \pm 0.3	2	0.3	0.1	0.33
Mangrove	<i>Avicennia</i> <i>marina</i>	Unimpacted Impacted	-26.7 \pm 2.2 -25.4 \pm 0.1	-28.8 \pm 0.6 -27.0 \pm 0.3	2	1.3	1.8	0.67
MPB		Unimpacted Impacted	-25.4 \pm 0.8 -20.9 \pm 1.2	-27.4 -20.7	1	4.5	6.7	-

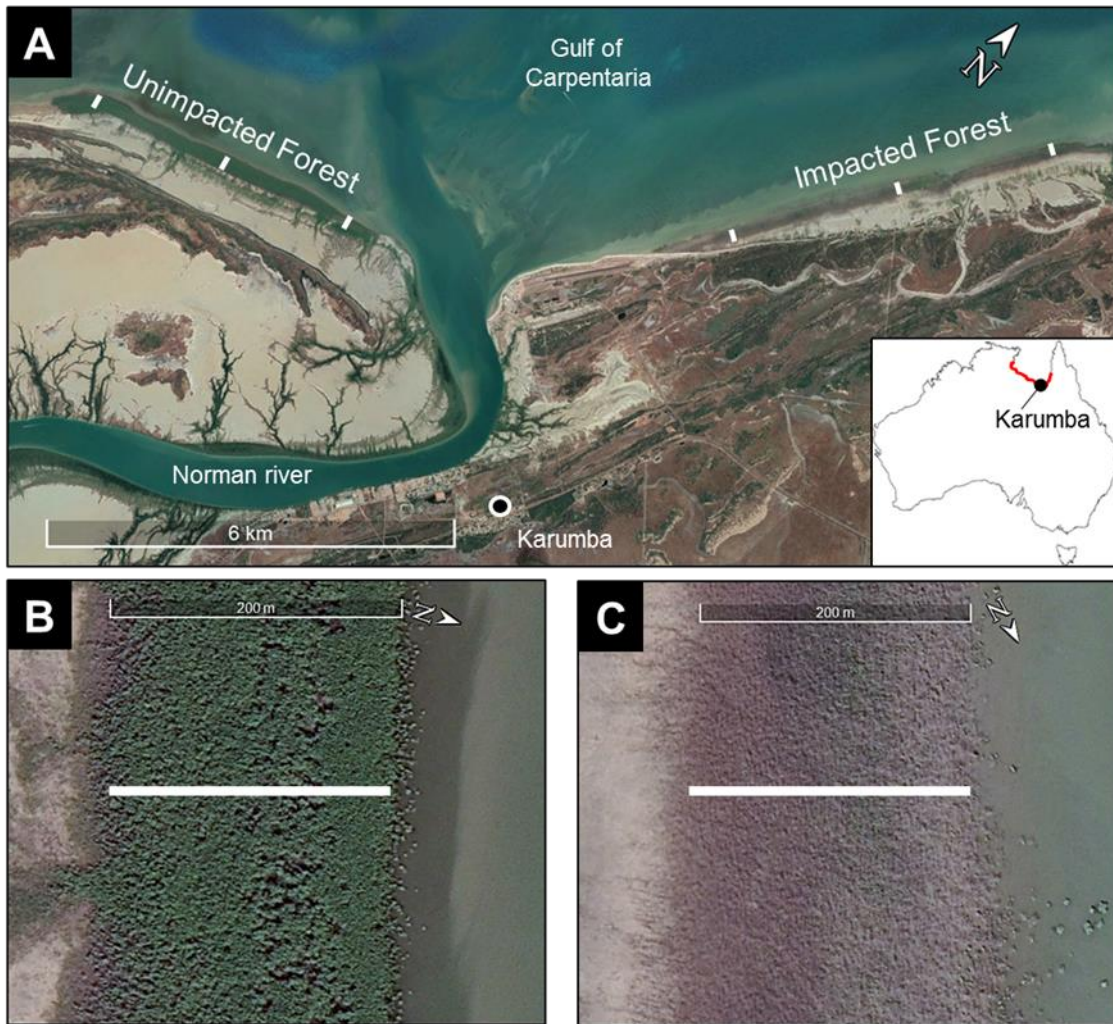


Figure 1. The study location at Karumba in the Gulf of Carpentaria, Queensland, Australia (-17.435572S, 140.844766E; image provided by Google Earth). (A) Three sampling transects within the unimpacted reference site and three within the impacted site (shown as a white line). (B, C) Representative transects from the unimpacted (B) and impacted (C) sites. Each transect was approximately 200m. Samples were collected along each transect from higher to lower intertidal zones. Red indicated mass dieback region.

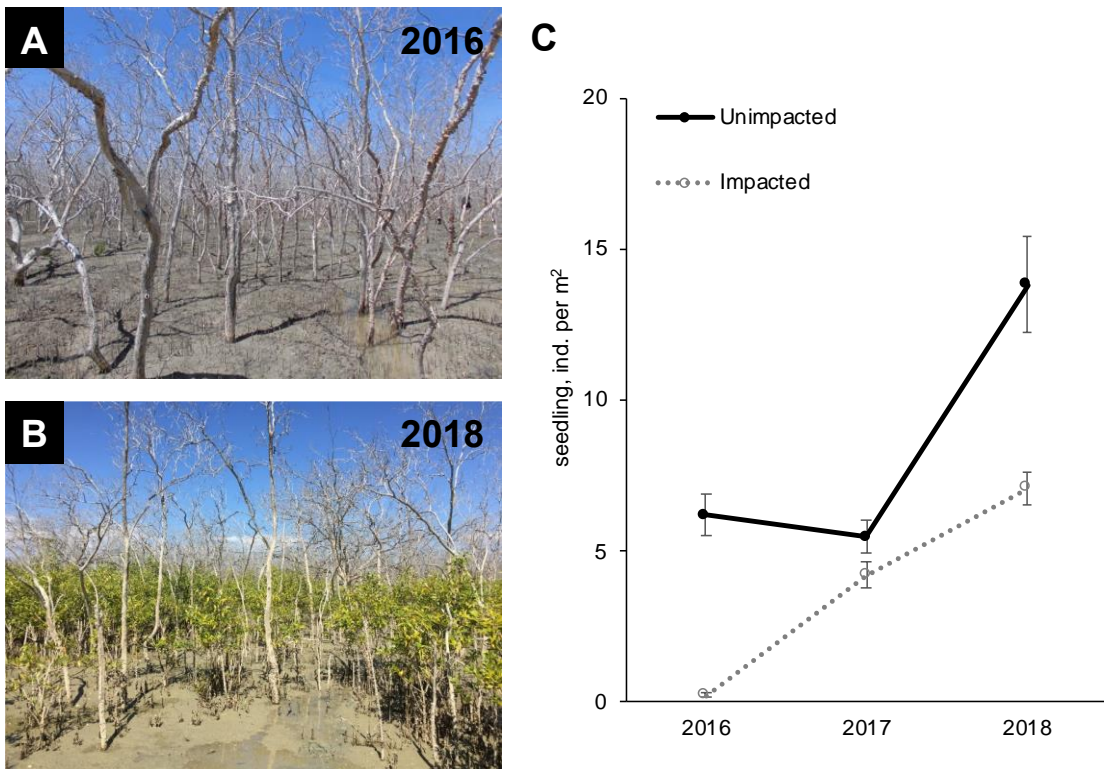


Figure 2. Recovery of mangrove vegetation at the impacted site during a two-year period from 2016 to 2018 (A and B; approx. 8 and 32 months, respectively after the dieback event). Seedling and sampling densities of mangrove species (mostly, *A. marina*) significantly increased in the impacted site (C; Table S1).

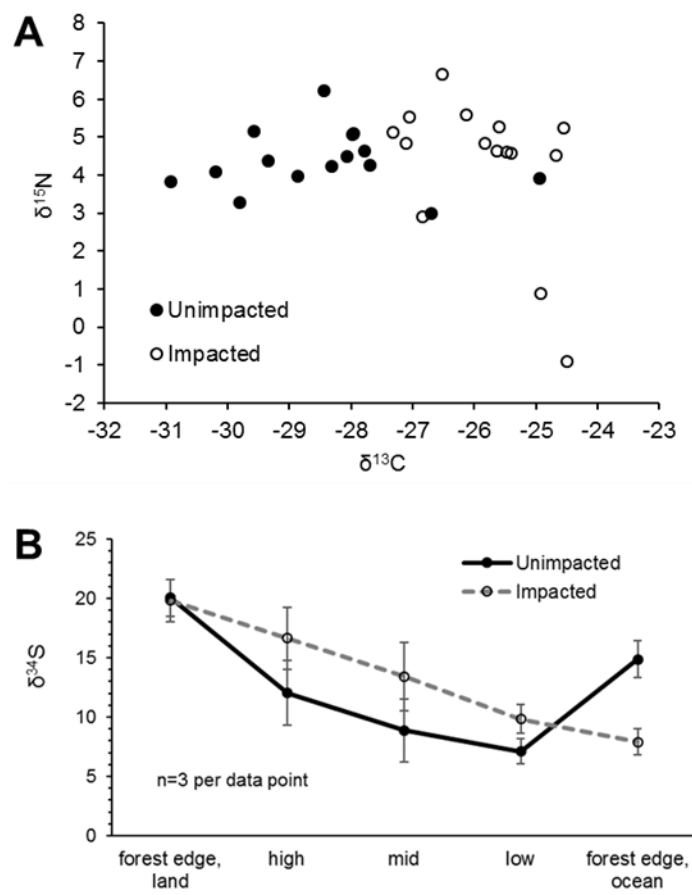


Figure 3. CNS isotopic compositions of green leaves of *A. marina* from the unimpacted and impacted sites. All samples were collected in 2018, 32 months after the dieback. (A) Leaf $\delta^{13}\text{C}$ and $\delta^{15}\text{N}$ values. (B) Leaf $\delta^{34}\text{S}$ values across the intertidal zones. Error values are SE.

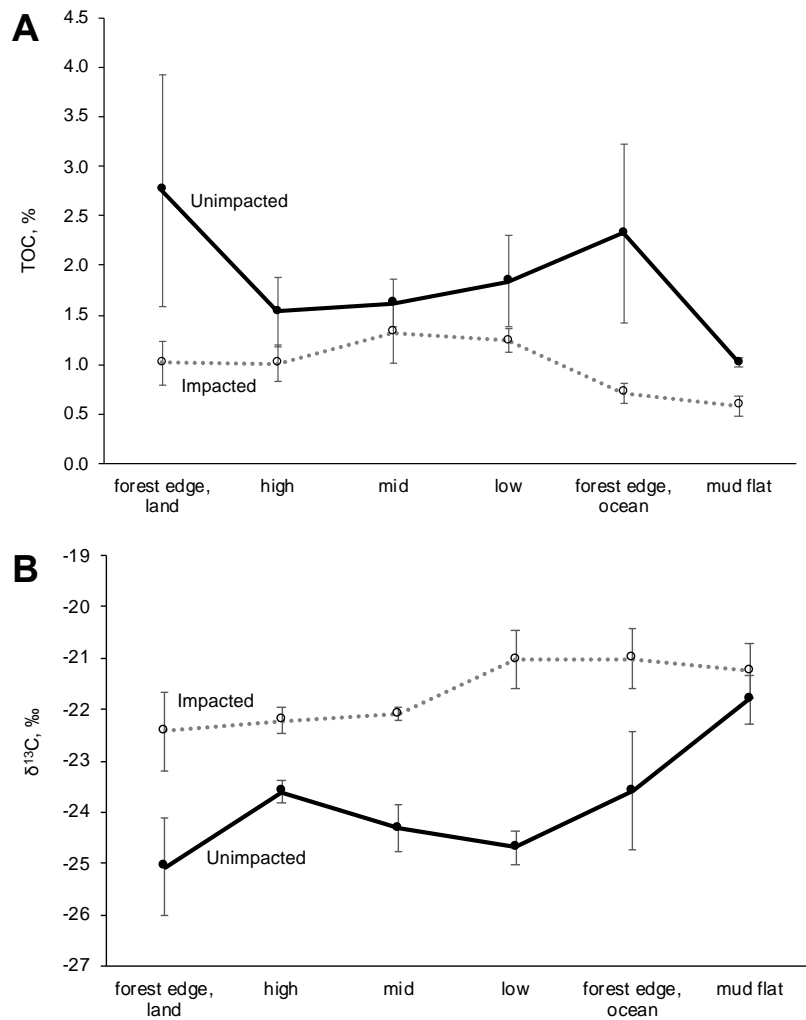


Figure 4. C elemental and isotopic compositions of surface (< 0.5 cm) sediment along the unimpacted reference transects vs impacted transects (n=3 per data point). All samples were collected in 2018, 32 months after the dieback. Error values are SE. (A) Sediment TOC, %. (B) Sediment $\delta^{13}\text{C}$ values, ‰.

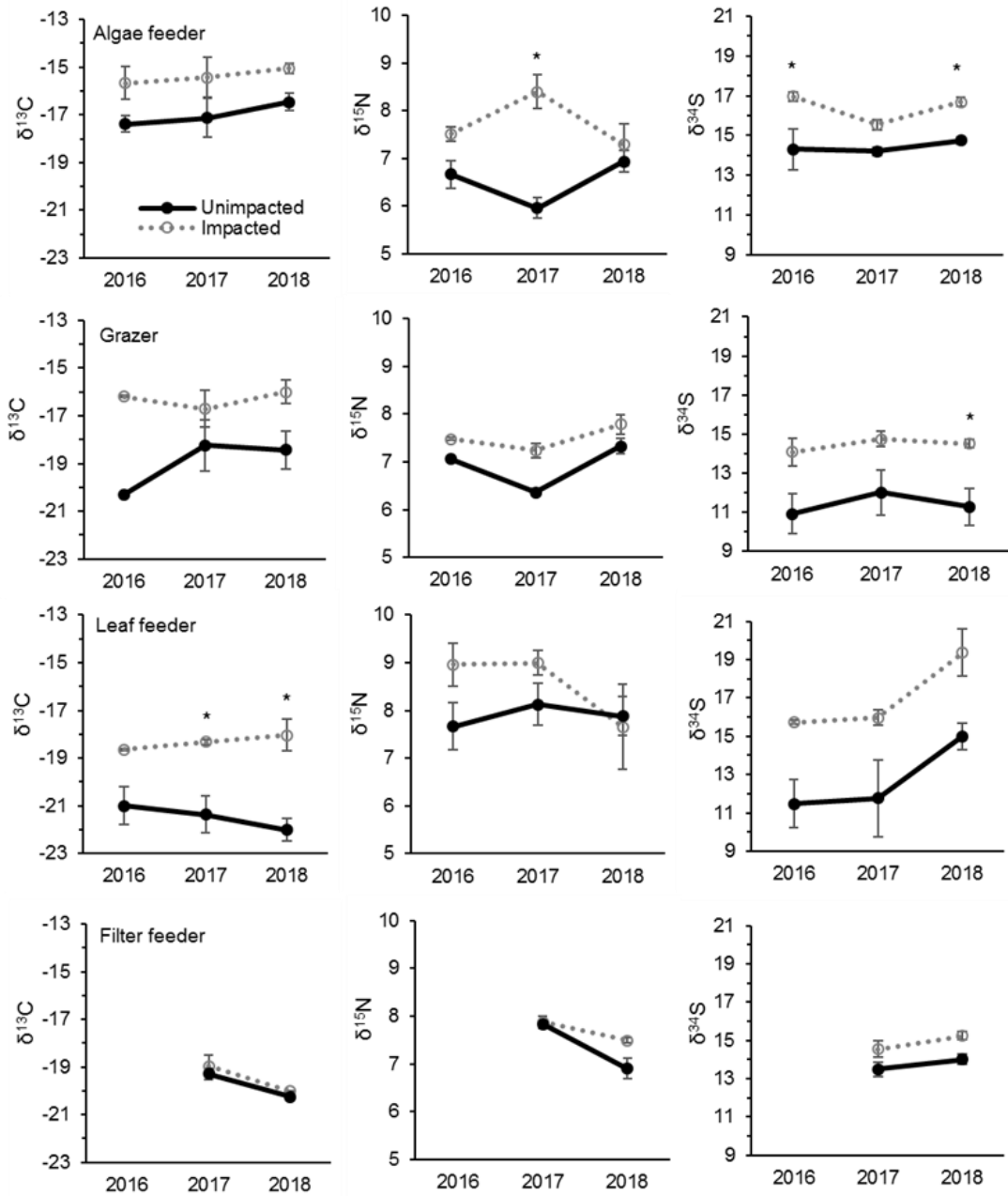


Figure 5. Changes in CNS isotopic compositions of mangrove macrofaunal groups with four different feeding modes from 2016, 2017 and 2018 (i.e. 8, 20 and 32 months after the event) between the unimpacted reference and impacted mangrove forest sites. Error bars are $\pm \text{SE}$ ($n=2$ to 6 per data point). (*) indicates a significant difference in the year. Mean $\pm \text{SE}$ values and sample sizes are also provided in Table S4.

675

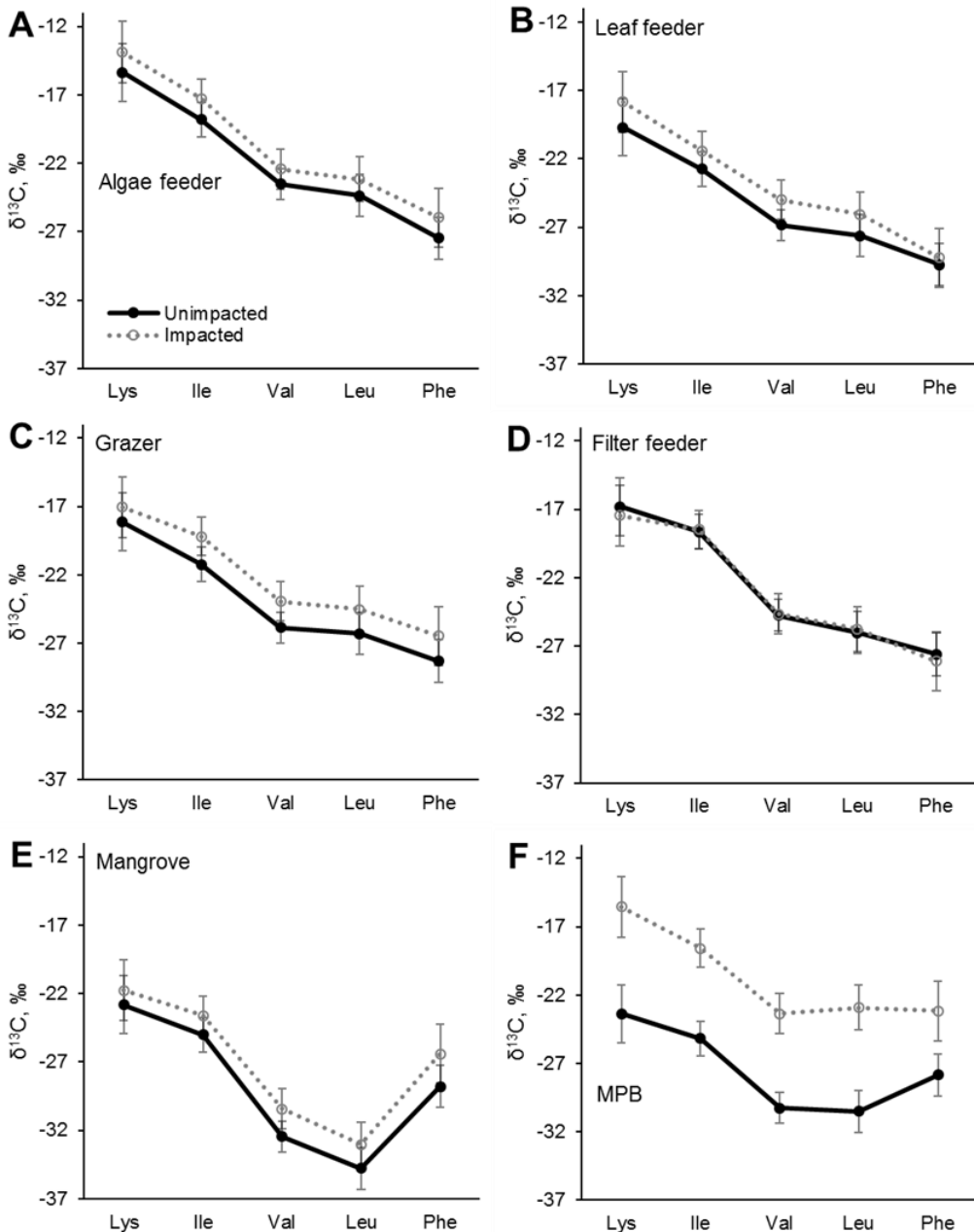


Figure 6. C isotopic compositions in essential amino acids (EAAs) for four mangrove consumer groups and resources including mangrove leaves (*A. marina*) and MPB from the unimpacted and impacted mangrove sites during 2017 (20 months after the dieback). While there are clear offsets in individual $\delta^{13}\text{C}_{\text{EAA}}$ values between the two forests, normalized $\delta^{13}\text{C}_{\text{EAA}}$ fingerprint patterns as per Larsen (2009) shown in Fig S1 did not differ (PERMANOVA $p > 0.05$, Table 3). Error bars show $\pm \text{SD}$. The data is provided in Table S5.

Disturbance legacies of the forest dieback



- Forest dieback due to extreme climatic events (impacted)
- $\delta^{13}\text{C}$ - weak C₃ plants signal (due to loss of mangroves)
 - $\delta^{15}\text{N}$ - Moderate to high (due to degradation and lower N fixation)
 - $\delta^{34}\text{S}$ - Moderate to high (lower sulfate reduction with a strong seawater sulfate signal)



- Healthy mangrove ecosystem (background)
- $\delta^{13}\text{C}$ - strong C₃ plants signal
 - $\delta^{15}\text{N}$ - Low to moderate (high N fixation)
 - $\delta^{34}\text{S}$ - Low to moderate (high sulfate reduction)

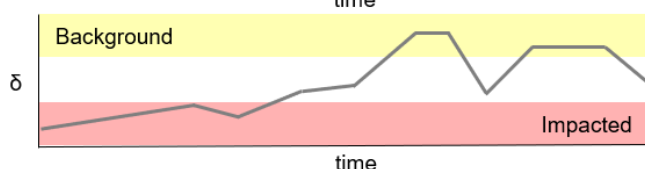
Predicted recovery scenarios with isotopic trajectories



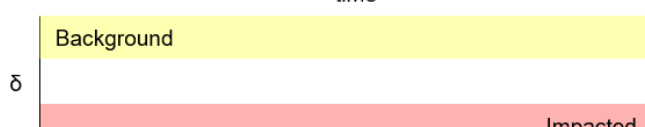
- (1) Recovery with no future perturbations
- Environmental conditions allow recolonisation
 - Recovery of $\delta^{13}\text{C}$, $\delta^{15}\text{N}$ and $\delta^{34}\text{S}$ to the background



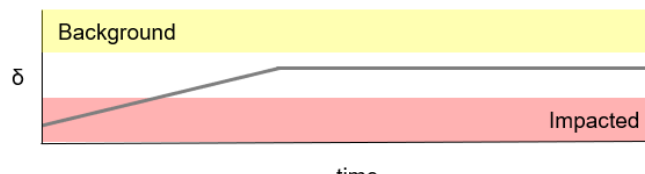
- (2) Recovery with future perturbations
- Mangrove recolonisation and recovery of $\delta^{13}\text{C}$, $\delta^{15}\text{N}$ and $\delta^{34}\text{S}$ driven by perturbations e.g. ENSO cycles



- (3) Habitat becomes unsuitable for recolonisation
- Conditions not allow recolonisation e.g. due to extreme climatic events
 - Transformed into intertidal mudflats
 - No recovery of isotopes



- (4) Incomplete recovery
- Reduced habitat size and/or recolonised by other plants such as saltmarshes
 - Incomplete recovery of $\delta^{13}\text{C}$, $\delta^{15}\text{N}$ and $\delta^{34}\text{S}$



685 **Figure 7.** A conceptual diagram showing the ecological and biogeochemical legacy of the mangrove forest dieback in the Gulf of Carpentaria and four predicted recovery scenarios of the mangrove ecosystem with isotopic trajectories (δ represents the isotope values of animals, plants and sediment).